ADVANCED FUNCTIONAL MATERIALS

DOI: 10.1002/adfm.200701340

Gold Nanoparticle–Colloidal Carbon Nanosphere Hybrid Material: Preparation, Characterization, and Application for an Amplified Electrochemical Immunoassay**

By *Rongjing Cui, Chang Liu, Jianming Shen, Di Gao, Jun-Jie Zhu,** and *Hong-Yuan Chen*

A rapid microwave-hydrothermal method has been developed to prepare monodisperse colloidal carbon nanospheres from glucose solution, and gold nanoparticles (AuNPs) are successfully assembled on the surface of the colloidal carbon nanospheres by a self-assembly approach. The resulting AuNP/colloidal carbon nanosphere hybrid material (AuNP/C) has been characterized and is expected to offer a promising template for biomolecule immobilization and biosensor fabrication because of its satisfactory chemical stability and the good biocompatibility of AuNPs. Herein, as an example, it is demonstrated that the as-prepared AuNP/C hybrid material can be conjugated with horseradish peroxidase-labeled antibody (HRP-Ab_2) to fabricate HRP-Ab_2-AuNP/C bioconjugates, which can then be used as a label for the sensitive detection of protein. The amperometric immunosensor fabricated on a carbon nanotube-modified glass carbon electrode was very effective for antibody immobilization. The approach provided a linear response range between 0.01 and 250 ng mL^{-1} with a detection limit of 5.6 pg mL^{-1}. The developed assay method was versatile, offered enhanced performances, and could be easily extended to other protein detection as well as DNA analysis.

1. Introduction

The development of nanoscience and nanotechnology has brought a great momentum to electrochemical bioassay. Analysts in this field are always enthusiastic in finding new materials with good biocompatibility for improving the behavior of bioassays. It has been reported that nanoparticle (NP)-based amplification platforms and amplification processes dramatically enhance the intensity of the electrochemical signal and lead to ultrasensitive bioassays.[1–3] Metal NPs, for example, were once directly used as electroactive labels to amplify the electrochemical detection of DNA and proteins.[4,5] Meanwhile, some nanomaterials, such as carbon nanotubes[6,7] and silicon nanoparticles[8–11] have been used as efficient carriers to load a large amount of electroactive species (enzyme, guanine, etc.) as reporters/markers for amplifying the detection of biomolecules. However, as-prepared nanomaterials usually have relatively inert surfaces, which makes surface modification almost unavoidable before use as supports.[12–15]

Recently, Li and coworkers[16] developed a controllable hydrothermal synthetic route to monodisperse colloidal carbon spheres in aqueous glucose solutions. The approach is an absolute 'green' method, and the synthetic procedure involves none of the organic solvents, initiators, or surfactants that are commonly used for the preparation of polymer micro- or nanospheres. The colloidal carbon spheres represent excellent candidates for application in bioassays by virtue of their high chemical stability, and the convenient and absolutely 'green' preparation method.[16] In particular, the as-formed colloidal spheres inherit large numbers of functional groups from the starting materials and have reactive surfaces, which facilitate loading with noble-metal nanoparticles and make it possible for further bioassay application.

In this work, we present a new method for the rapid synthesis of colloidal carbon spheres in aqueous glucose solutions by a microwave-hydrothermal technique. Citrate-stabilized gold nanoparticles (AuNPs) are assembled on the surface of colloidal carbon spheres to fabricate a core–shell hybrid material by the self-assembly approach. This material retains the colloids' stability and inherits the advantages from its parent materials, such as good solubility and dispersibility in water. Furthermore, since carbon is far more stable than polymers with respect to high-temperature stability and resistance to acids, bases, and solvents, these hybrid structures should have superior advantages over noble-metal nanoparticle-decorated polymer spheres in fields such as catalysis or protein and DNA detection.

The advantages of the core–shell AuNP-colloidal carbon sphere (AuNP/C) hybrids make them suitable for biomolecule loading, e.g., with horseradish peroxidase-labeled antibody

[*] Prof. J.-J. Zhu, R. J. Cui, C. Liu, J. M. Shen, D. Gao, Prof. H. Y. Chen
MOE Key Laboratory of Analytical Chemistry for Life Science
School of Chemistry and Chemical Engineering, Nanjing University
Nanjing 210093 (P. R. China)
E-mail: jjzhu@nju.edu.cn

[**] This project was supported by the National Natural Science Foundation of China (20635020, 20575026, and 20521503) and the National Basic Research Program of China (2006CB933201). We are grateful to the financial support of the European Community Sixth Framework Program through a STREP grant to the SELECTNANO Consortium, Contract No. 516922.

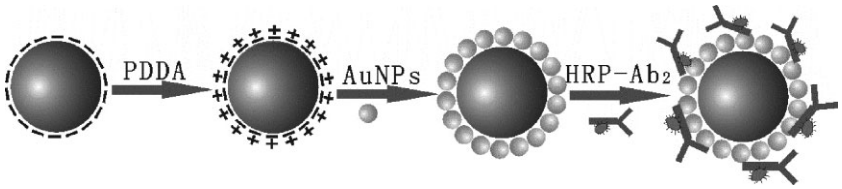

Scheme 1. Assembly procedure for multifunctional HRP-Ab_2-AuNP/C bioconjugates.

molecules (HRP-Ab_2) (Scheme 1). The resulting HRP-Ab_2-functionalized AuNP/C (HRP-Ab_2-AuNPs/C) bioconjugates could find application in the electrochemical detection of protein. Herein, we pursued a multi-label strategy that provided the advantages of enhanced sensitivity and selectivity by virtue of a 'sandwich-type' immunoassay. The amplified sensitivity was enhanced by using bioconjugates that feature a HRP-Ab_2-AuNP/C hybrid material (Scheme 2). To prepare the biosensor, the Ab_1 molecules were immobilized on a carbon nanotube (CNT)-modified glass carbon electrode (GCE), which constructed an effective antibody immobilization matrix and made the immobilized immunocomponents maintain high stability and bioactivity. To the best of our knowledge, this is the first time that the self-assembly of HRP-Ab_2-AuNP/C conjugates have been used as an amplified platform in an immunoassay. It might be an effective candidate for the detection of protein or DNA because it offers a versatile, practical, and convenient protocol in clinical diagnoses.

2. Results and Discussion

2.1. Preparation and Characterization of the AuNP/C Hybrid Material

The microwave-hydrothermal technique is a useful tool to decompose chemicals by the creation of friction and collisions of the molecules under high temperature. Some studies have shown that the synthesis of nanoparticles with the technique is generally quite fast, simple, and energy efficient compared with conventional hydrothermal synthesis.[17,18] To the best of our knowledge, there are no reports on the preparation of highly stable and uniformly sized colloidal carbon nanospheres by the technique.

Carbon spheres were prepared from glucose under microwave-hydrothermal conditions at 170 °C, which is higher than the normal glycosidation temperature and leads to aromatization and carbonization.[19] The FTIR spectrum as shown in Figure 1 was used to identify the functional groups present after the microwave-hydrothermal treatment. In the spectra of colloidal carbon spheres, the characteristic peaks at 1710 and 1620 cm^{-1} correspond to C=O and C=C vibrations, respectively, which is a result of the aromatization of glucose during the treatment. The peaks in the range 1000–1300 cm^{-1}, which include the C–OH stretching and OH bending vibrations, imply the existence of large numbers of residual hydroxy groups. Partially dehydrated residues in which reductive hydroxy groups (OH) and aldehyde groups (CHO) are covalently bonded to the carbon frameworks improve the hydrophilicity and stability of the nanospheres in aqueous systems, and greatly widen their potential applications in biochemistry, diagnostics, and drug delivery.[16] The controlled assembly of metal nanoparticles on the colloidal carbon spheres is important for these applications.

The layer-by-layer (LBL) assembly of oppositely charged polyelectrolytes and nanoparticles has been widely studied as an effective route to fabricate multifunctional hybrid materials.[20,21] Herein, AuNPs were anchored to the surface of colloidal carbon nanospheres by a simple and versatile scheme of electrostatic adsorption. As expected, the original colloidal carbon spheres in aqueous solution (pH 7.0) had a negative ξ-potential of −49.4 mV. Thus, the colloidal carbon spheres prepared are negatively charged and are electrostatically attracted to the cationic polyelectrolyte poly (diallyldimethylammonium chloride) (PDDA), which provides a homogeneous distribution of positive charges. The presence of a layer of adsorbed positively charged PDDA on the colloidal carbon spheres causes a reversal in ξ-potential to positive values (+38.20 mV). These positive charges ensure the efficient adsorption of negatively charged AuNPs onto the surface of colloidal carbon spheres by means of electrostatic interactions. Several experimental techniques can be employed to monitor the formation of a Au colloidal layer deposited on colloidal carbon spheres.

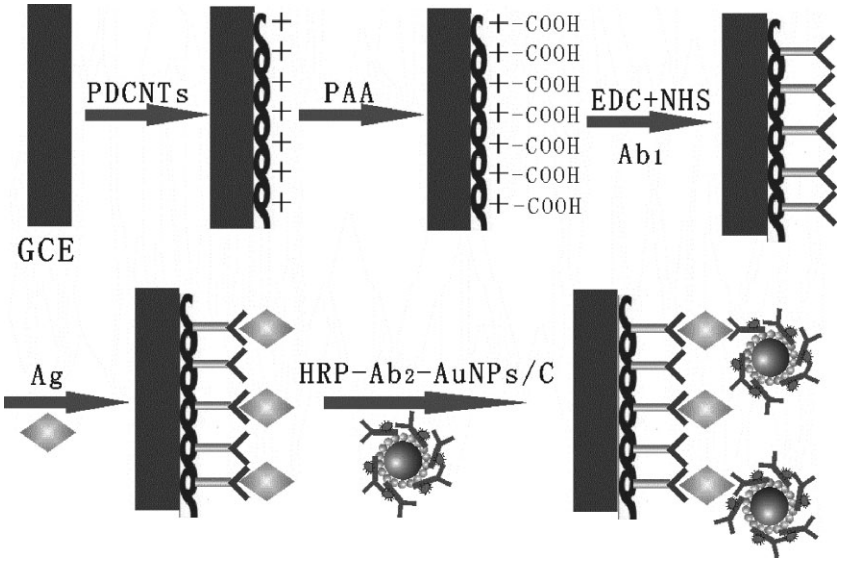

Scheme 2. The analytical procedure of PAA/PDCNT-modified immunosensor using HRP-Ab_2-AuNP/C bioconjugates.

Figure 2 shows the typical transmission electron microscopy (TEM) and field-emission scanning electron microscopy (FESEM)

ADVANCED FUNCTIONAL MATERIALS

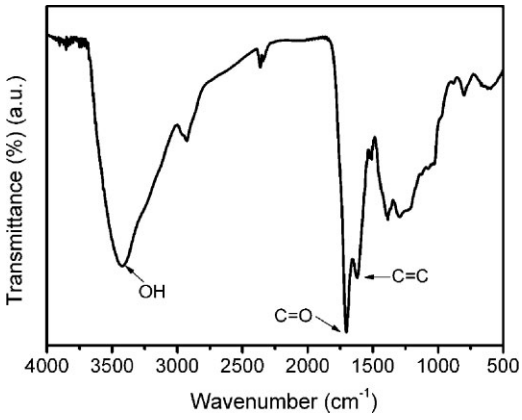

Figure 1. FTIR spectrum of colloidal carbon nanospheres.

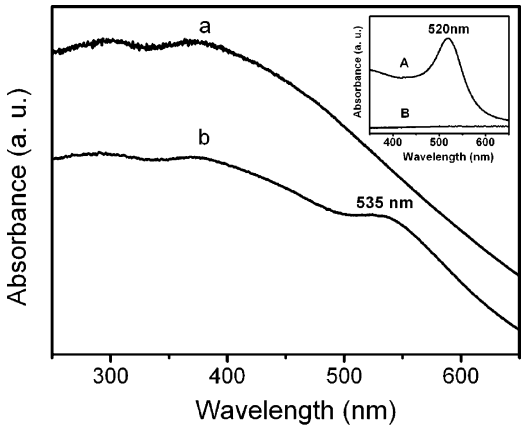

Figure 3. UV-Vis spectra of a) colloidal carbon spheres and b) AuNP/C hybrids. Upper insets show the UV-vis spectra of the as-prepared colloidal gold solution (A) and the gold solution after reaction with colloidal carbon spheres and centrifugation (B).

images of the colloidal carbon nanospheres and the AuNP/C hybrid material. The obtained colloidal carbon nanospheres with an average diameter of 250 nm are uniform in size and morphology. The numerous individual dark nanodots spread along the grey nanospheres in Figure 2b and the corresponding outside particles in Figure 2d are AuNPs, which indicates that well-dispersed AuNPs decorate the colloidal carbon surface quite uniformly. This indicates that PDDA plays a key role in the attachment; it acts as a bridge to connect the AuNPs to the colloidal carbon spheres.

UV-Vis absorption spectra of the PDDA-modified colloidal carbon nanospheres and the AuNP/C hybrid materials are shown in Figure 3. The upper insets show the UV-vis spectra of the as-prepared colloidal gold solution (A) and the AuNP solution after reaction with colloidal carbon nanospheres and centrifugation (B). The characteristic peak of citrate-stabilized colloidal AuNPs appears at 520 nm, which was caused by the surface plasmon resonance. A great loss in the intensity of the surface plasmon resonance at 520 nm was found after the AuNPs were deposited, which indicates that the AuNPs could be efficiently adsorbed onto the surface of the colloidal carbon spheres. From the loss of intensity at 520 nm in this figure, we made a rough estimate of 3.6% for the mass loading of colloidal carbon spheres with AuNPs. Compared with the spectrum of pure colloidal carbon spheres (curve a), a new absorption band centered at 535 nm is observed in the spectrum of the AuNP/C hybrids (curve b), which indicates the capture of AuNPs. The shift in the resonance wavelength was attributed to interparticle plasmon coupling, a phenomenon observed even when just a few AuNPs or nanorods were clustered together.[22,23] The result suggests that some of the surface-modified AuNPs were in close proximity with each other but were not agglomerated, as evidenced by the TEM images.

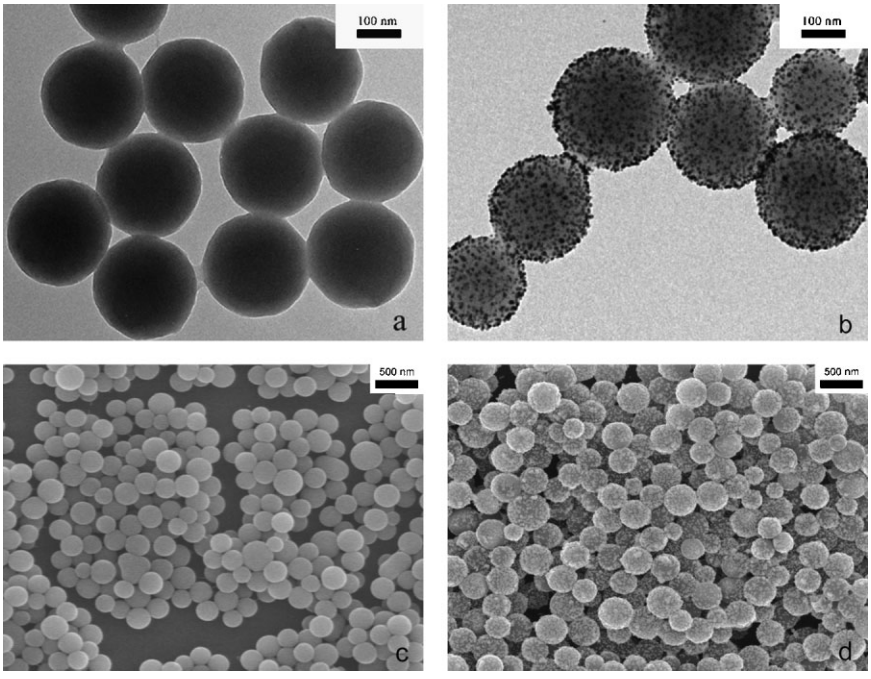

Figure 2. a) TEM and c) SEM images of colloidal carbon nanospheres, and b) TEM and b) SEM images of the AuNP/C hybrids.

X-ray photoelectron spectroscopy (XPS) was also used to characterize the samples in a wide scan (Fig. 4A). Compared with the spectrum of pure colloidal carbon nanospheres (curve a in Fig. 4A), a new and weak peak at 402 eV is observed in the spectrum of the PDDA-modified colloidal carbon spheres. The peak position corresponds to N 1s, which indicates the presence of PDDA. In curve c of Figure 4A, an additional peak at 84 eV, which represents Au 4f, is observed and shows the existence of AuNPs in

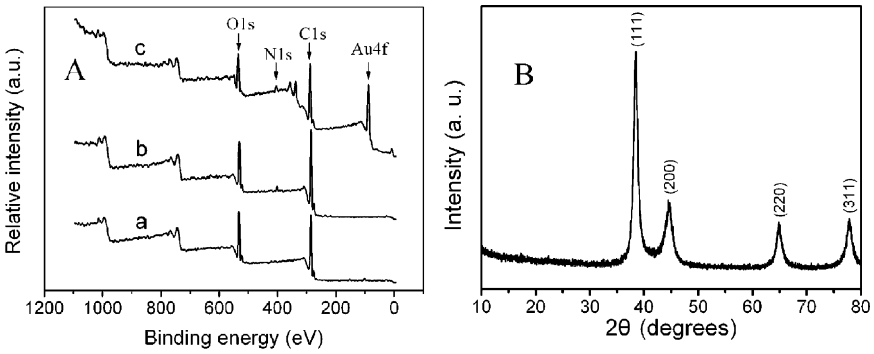

Figure 4. A) XPS spectra of a) pure colloidal carbon nanospheres, b) PDDA-modified colloidal carbon spheres, and c) AuNP/C hybrid material. B) XRD pattern of AuNP/C hybrid material.

the hybrids. The AuNP/C hybrids exhibit an X-ray powder diffraction (XRD) pattern of a typical face-centered-cubic (fcc) lattice structure as shown in Figure 4B. The strong diffraction peaks at the Bragg angles of 38°, 43°, 65°, and 77° correspond to the (111), (200), (220), and (311) planes of the Au crystal. The results also indicate that the AuNPs were immobilized in a well-dispersed way on the outer surface of the colloidal carbon nanospheres.

In addition, by choosing different kinds of polyelectrolytes, the surfaces of colloidal carbon nanospheres can be tailored to be negatively or positively charged, some other nanoparticles such as semiconductor nanocrystals or magnetic nanoparticles can be selectively attached to the surface of colloidal carbon nanospheres. These nanoparticle-decorated carbon nanosphere heterostructures can be used in catalytic, electronic, optical, and magnetic applications. To demonstrate the potential application in immunoassay of the AuNP/C hybrids, the AuNP/C hybrid materials were bioconjugated with HRP-Ab_2 to form HRP-Ab_2-AuNP/C bioconjugates. On the basis of the HRP-Ab_2-AuNP/C bioprobes, a novel and sensitive amperometric immunosensor has been developed.

2.2. Utilization of Biofunctionalized HRP-Ab_2-AuNP/C Bioconjugates for Immunoassay

2.2.1. HRP-Ab_2-AuNP/C Bioconjugates

A biomaterial bearing multiple HRP-Ab_2 labels attached to AuNP/C surfaces was first developed for multi-label amplification to enhance sensitivity. HRP-Ab_2 was linked with the AuNP/C composites by modification of a literature procedure.[24,25] After the HRP-Ab_2 adsorption, the HRP-Ab_2 conjugated AuNP/C composites were precipitated by centrifugation. The HRP-Ab_2 concentrations before adsorption and the HRP-Ab_2 concentration that remained in the supernatant after the antibody adsorption were determined by UV-vis spectrophotometric measurements at 280 nm. The difference in the amount of HRP-Ab_2 before and after adsorption was calculated and represented the amount of HRP-Ab_2 adsorbed onto the AuNP/C hybrid surfaces. The sum amount of HRP-Ab_2 in the stock HRP-Ab_2-AuNP/C dispersion was estimated to be 15.32 μg mL^{-1}.

2.2.2. Preparation and Characterization of the Immunosensor

Electron impedance spectroscopy (EIS) has been reported as an effective method to monitor the features of a surface to allow the understanding of chemical transformations and processes associated with the conductive electrode surface.[26] The impedance spectra include a semicircle portion and a linear portion, the semicircle portion at higher frequencies corresponds to the electron-transfer limited process, and the linear part at lower frequencies corresponds to the diffusion process. The semicircle diameters correspond to the electron-transfer resistance (R_{et}). Figure 5 shows the Nyquist plots of EIS for the bare GCE, PDDA-CNT (PDCNT)/GCE, poly(acrylic acid) (PAA)/PDCNT/GCE, and Ab_1/PAA/PDCNT/GCE. At a bare GCE, the redox process of the $[Fe(CN)_6]^{3-/4-}$ probe showed an electron transfer resistance of about 81 Ω (curve a). The PDCNT-modified GCE showed a much lower resistance for the redox probe (curve b), which implies that PDCNTs are an excellent electric conducting material and accelerate the electron transfer. After the PDCNT-modified electrode was adsorbed with PAA, the electron transfer resistance increased (curve c), which showed that the self-assembled layers with COO^- terminal groups on the electrode surface generated a negatively charged surface that reduced the ability of the redox probe to access the layer.[27] Subsequently, the Ab_1 molecules were combined covalently on the PAA/PDCNT-modified electrode and the R_{et} increased again (curve d). The result was consistent with the fact that the protein layer on the electrode generates a barrier for electron transfer. It should be

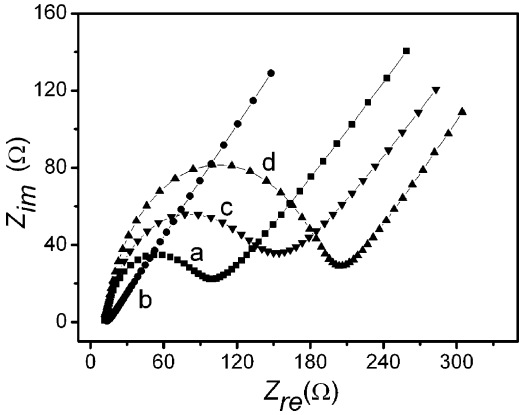

Figure 5. EIS of bare (a), PDCNT (b), PAA/PDCNT (c), and Ab_1/PAA/PDCNT (d) modified GCEs in 0.10 M KNO_3 containing 2.0×10^{-3} M $K_3[Fe(CN)_6]/K_4[Fe(CN)_6]$.

ADVANCED FUNCTIONAL MATERIALS

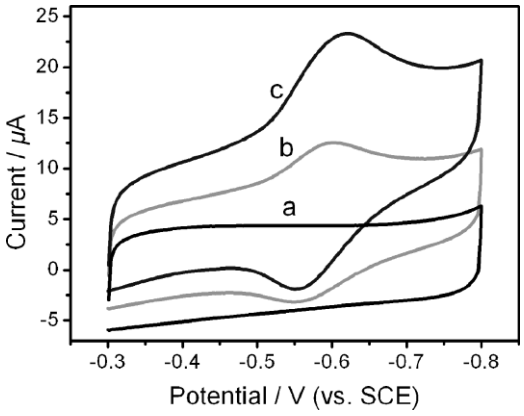

Figure 6. Cyclic voltammograms of a) Ab_1/PAA/PDCNT/GCE, b) HRP-Ab_2-Ag complexes/PAA/PDCNT/GCE, c) HRP-Ab_2-AuNP/C-Ag complexes/PAA/PDCNT/GCE at in 0.1 M pH 7.0 PBS that contains 2.0×10^{-3} M *o*-phenylenediamine and 4.0×10^{-3} M H_2O_2. Scan rate: 100 mV s^{-1}.

mentioned that the prepared PDCNT-modified electrodes were found to be very stable, which was illustrated by the redox process of $[Fe(CN)_6]^{3-/4-}$ in solution phase: the redox peak currents were essentially unchanged after continuously cycling the electrodes for 100 cycles. Thus, the PDCNT-modified GCE constructed an effective antibody immobilization matrix to immobilize biomolecules with high stability and bioactivity.

It could be verified that the amperometric response of the immunosensor depended on the immunocomplexes by cyclic voltammetry (CV) analysis (Figure 6). No amperometric response was observed for the Ag/Ab_1/PAA/PDCNT/GCE over the working potential range in 0.1 M pH 7.0 phosphate-buffered saline (PBS) that contained *o*-phenylenediamine and H_2O_2 (curve a). After incubation with conventional HRP-labeled Ab_2, the immunosensor showed a pair of stable redox peaks, the anodic and cathodic peak potentials were −0.551 and −0.601 V (vs. SCE), respectively (curve b), which corresponded to the redox potential of 2,2′-diaminoazobenzene, the enzymatic product.[28] When the immunosensor was incubated with HRP-Ab_2-AuNP/C bioconjugates, the pair of redox peaks of the enzymatic product increased greatly (curve c), which indicates that AuNP/C hybrids provide a larger number of active sites for the binding of HRP-Ab_2 in the enzymatic reaction to obtain a sensitive immunoassay.

The sandwich immunoassay of HIgG was further examined using HRP-Ab_2-AuNP/C bioconjugates and HRP-Ab_2 as labels, respectively. Figure 7A shows the typical differential pulse voltammetrics (DPVs) obtained after the sandwich immunoreaction for different concentrations of HIgG using HRP-Ab_2-AuNP/C bioconjugates. In a control experiment (curve b), the immunosensor was taken through the full procedure without exposure to Ag, the peak current is a little higher than the background current (curve a), which might be caused by the physical adsorption of the HRP-Ab_2-AuNP/C bioconjugates on the GCE surface and the direct reduction of hydrogen peroxide at the Ab_1/PAA/PDCNT/GCE. However, the DPV signals were enhanced in the presence of different concentrations of HIgG analytes (from c to h). One observed that the voltammetric peaks appeared at −0.596 V, and the peak current increased with the increase in the concentration of HIgG. Figure 7B shows the typical DPV detection of HIgG using the HRP-Ab_2 as a label. The voltammetric peaks were well defined and the intensity was proportional to the concentration of the corresponding HIgG (from curve b to g). However, the signal intensity was greatly decreased compared with the HRP-Ab_2-AuNP/C label. Figure 7C shows the plot of background subtracted peak current versus the logarithm of the concentration of HIgG using HRP-Ab_2-AuNP/C bioconjugates (a) and HRP-Ab_2 (b) as labels. It could be seen from curve a in Figure 7C that the current linearly increased with the increase of the logarithm of the concentration of the HIgG over the 0.01–250 ng mL^{-1} range. The limit of detection for this immunosensor (based on $S/N = 3$) was estimated to be 5.6 pg mL^{-1}. For the assay using HRP-Ab_2 (curve b in Fig. 7C), a linear detection range for the logarithm of the concentration of HIgG was observed from 1.2 to 500 ng mL^{-1} with the detection limit of 0.49 ng mL^{-1}. The result indicated that the sensitivity of detection using the HRP-Ab_2-AuNP/C conjugates was much higher than that obtained using HRP-Ab_2. The analysis sensitivity enhancement achieved using HRP-Ab_2-AuNP/C bioconjugates was a result of a higher

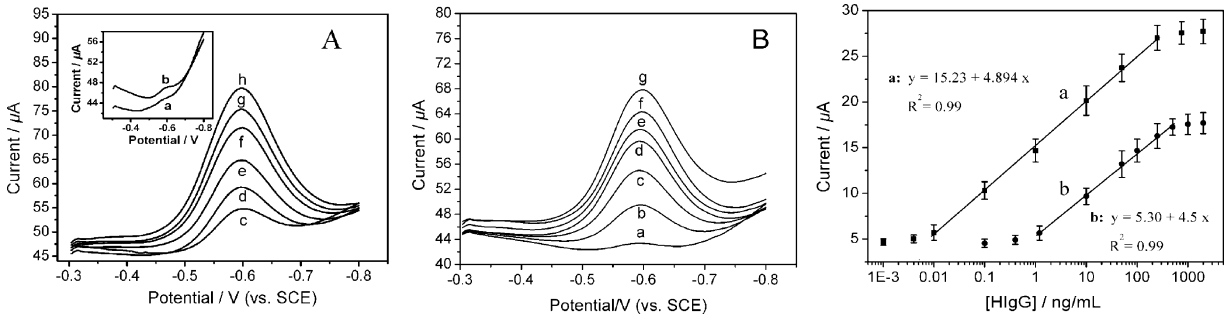

Figure 7. A) Typical DPV of electrochemical immunoassay using HRP-Ab_2-AuNP/C conjugates with different concentrations of HIgG. Curve a is from the Ab_1/PAA/PDCNT-modified GCE; Curve b is from the control electrode (in the absence of HIgG). Curves c–h are from the electrodes incubated with different concentrations of HIgG (0.01, 0.1, 1.0, 10.0, 50, and 250 ng mL^{-1} of HIgG, respectively). B) Typical DPV of electrochemical immunoassay using HRP-Ab_2 with different concentration HIgG from a to g (0, 1.2, 10, 50, 100, 250, and 500 ng mL^{-1} of HIgG, respectively). C) Calibration plots of background-subtracted peak current versus the logarithm of the concentration of HIgG using HRP-Ab_2-AuNP/C (a) and HRP-Ab_2 (b) as labels.

number of HRP molecules. However, the resulting detection limit decreased because of a lower non-specific signal. This could be explained only by the fact that, during the washing steps, the non-specific interactions could be eliminated more easily when the antibody was attached to AuNP/C than when it was alone. That placed the non-specific signal at a value lower than that at which it should be considering the signal enhancement.

The demonstrated detection limit of HIgG was well below those obtained from most of the presently available enzyme-linked immunosorbent assays[29] (ELISA, 40 pg mL^{-1}). Our results also strongly suggest the presented method as being a very promising analytical tool because of its high sensitivity, low cost, rapid response, and low power requirements. Recently, various electrochemical bioassays[30–33] have been reported, including electrochemical immunosensor and electrochemical DNA sensors, and some of the assays using amplification techniques and the aptamer-protein recognition method have shown high sensitivity. However, most of these assays, unfortunately, either are costly, laborious, and time consuming, or have some special requirements. These limit the application of those bioassay techniques and make them unfit for fast determination of the analyte. We have demonstrated that the combination of HRP-Ab_2-functionalized AuNP/C conjugates and Ab_1/PAA/PDCNT-modified immunosensor yield an analytically attractive performance. This approach can be easily extended to other protein detection schemes as well as in DNA analysis.

2.2.3. Specificity, Precision, Reproducibility, and Stability of the Immunosensor

Specificity is an important criterion for any analytical tool. Other proteins such as bovine serum albumin (BSA), C-reactive protein (CRP), and goat IgG were used to evaluate the selectivity of the sensor. The current values obtained for each interfering substance at a concentration of 50 ng mL^{-1} in the presence of 10 ng mL^{-1} of HIgG were used as an indicator for the sensor selectivity in comparison with the HIgG reading alone. The results of the interference study are listed in Table 1. They do not cause interference under the experimental conditions. The intra-assay precision was estimated by assaying one HIgG level for five replicate measurements. The inter-assay precision, or the fabrication reproducibility, was estimated by determining the HIgG level with five immunosensors made at the same GCE independently. The relative standard deviations (RSDs) of the intra- and interassay were 7.6% and 8.6% at the HIgG concentration of 10 ng mL^{-1}. After the biosensor was used three times, the analytical performances did not show an obvious decline, which demonstrates that the immunosensor possessed good stability.

Table 1. Possible interferences tested with the immunosensor.

Possible interferences	Current ratio [a]
BSA	0.99
CRP	1.02
goat IgG	1.03

[a] Ratio of currents for a mixture that contains 50 ng mL^{-1} of interfering substance and 10 ng mL^{-1} of HIgG compared with that for 10 ng mL^{-1} of HIgG.

Table 2. Comparison of serum HIgG levels determined using two methods.

Serum samples	Immunosensor [a] [ng mL^{-1}]	ELISA [a]	Relative deviation [%]
1	0.156	0.145	7.6
2	1.25	1.35	−7.4
3	65.6	70.5	−7
4	201.2	208.9	−7.8

[a] The average value of three successive determinations.

2.2.4. Application of the Immunosensor in Human Serum

The feasibility of the immunoassay system for clinical applications was investigated by analyzing several real samples, in comparison with the ELISA method. These serum samples were diluted to different concentrations with PBS of pH 7.0. Table 2 describes the correlation between the partial results obtained by the proposed immunosensor and the ELISA method. It obviously indicates that there is no significant difference between the results given by the two methods, that is, the proposed biosensor could be satisfactorily applied to the clinical determination of HIgG levels in human plasma.

3. Conclusion

Colloidal carbon spheres have been successfully synthesized by using a microwave-hydrothermal method. The synthesis is convenient, rapid, and the as-formed colloidal spheres inherit functional groups from the starting material and have reactive surfaces, which facilitate loading with AuNPs on the surface by self-assembly technology. The resulting multifunctional AuNP/C hybrids have been used for HRP-Ab_2-AuNP/C bioconjugate assembly and immunosensor fabrication to evaluate their feasibility in bioelectroanalysis. Thus, a novel electrochemical immunoassay for the detection of HIgG based on a HRP-Ab_2-functionalized AuNP/C hybrid nanomaterial label has been developed. This method is versatile, selective, and reproducible for protein analysis and the work demonstrates the application potential of the AuNP/C hybrid material in bioassay.

4. Experimental

Chemicals: Glucose (analytical purity) was purchased from Beijing Chemical Reagent Factory. Chloroauric acid ($HAuCl_4 \cdot 4H_2O$) and trisodium citrate were obtained from Shanghai Reagent Company (Shanghai, China). Poly(diallyldimethylammonium chloride) (PDDA, 20%, w/w in water, MW = 200 000–350 000), poly(acrylic acid) (PAA, 35%, w/w in water, MW = 100 000), 1-ethyl-3-(3-dimethylaminopropyl) carbodiimide hydrochloride (EDC), *N*-hydroxysuccinimide

ADVANCED FUNCTIONAL MATERIALS

(NHS), lyophilized 99% bovine serum albumin (BSA), and Tween-20 were from Sigma/Aldrich. Multi-walled carbon nanotubes (CNTs, CVD method, purity > 95%, diameter 30–60 nm, length 0.5–15 μm) were purchased from Nanoport. Co. Ltd (Shenzhen, China). Human IgG (HIgG), goat anti-human IgG (Ab_1), and HRP-labeled monoclonal mouse anti-human IgG (HRP-Ab_2) were purchased from Zhengzhou Chuangsheng Biochemical Reagents (Zhengzhou, China). Triethanolamine (TEA), *o*-phenylenediamine, and H_2O_2 of analytical grade were from Shanghai Biochemical Reagent Company (China). All other reagents were of analytical reagent grade and used without further purification. PBS (0.1 M) with various pH was prepared by mixing stock solutions of NaH_2PO_4 and Na_2HPO_4, and then adjusting the pH with 0.1 M NaOH and H_3PO_4. Doubly distilled water was used throughout the experiments.

Preparation of AuNPs and Colloidal Carbon Spheres: AuNPs were prepared according to the literature [34] by adding a sodium citrate solution to a boiling $HAuCl_4$ solution. Colloidal carbon spheres were prepared by a microwave-hydrothermal route. All the microwave-assisted hydrothermal reactions were conducted in a microwave-accelerated reaction system MARS-5 (CEM, USA). Briefly, 5 g of glucose was dissolved in 40 mL of water to form a clear solution. The mixed aqueous solution was treated at 170 °C and 180 psi for 20 min in a reaction vessel lined with Teflon. The microwave-accelerated reaction system was operated at a power of 200 W. The brown products were isolated by three cycles of centrifugation/washing/redispersion in water and oven-dried at 80 °C for more than 4 h.

Preparation of AuNP/C Hybrids: The purified colloidal carbon spheres were functionalized with PDDA. First, colloidal carbon spheres were dispersed into an aqueous solution of 0.20% PDDA that contained 20×10^{-3} M Tris and 20×10^{-3} M NaCl and the resulting dispersion was stirred for 20 min to give a homogeneous brown suspension. Residual PDDA was removed by high-speed centrifugation and the complex was rinsed with water at least three times. The colloidal carbon spheres (0.06 g) were dispersed in 50 mL of the Au colloid solution and stirred for 20 min. After centrifugation, the light-purple AuNP/C composites were obtained; the supernatant liquor was colorless. The composites were further washed with distilled water three times and redispersed in 50 mL of a 50×10^{-3} M pH 9.0 Tris-HCl solution.

The morphologies of the colloidal carbon nanospheres and AuNP/C hybrid spheres were observed by field-emission scanning electron microscopy (FESEM, JEOL JSM-6340 F) and transmission electron microscopy (TEM, JEOLJEM-200CX). X-ray photoelectron spectroscopy (XPS) was carried out on an ESCALAB MK II X-ray photoelectron spectrometer. All Fourier-transform infrared (FTIR) spectroscopic measurements were performed on a Bruker model VECTOR22 Fourier-transform spectrometer using KBr pressed disks. UV-Vis and diffuse reflectance (DRS) spectra were recorded on a Shimadzu UV-3600 recording spectrophotometer at room temperature. Zeta potential analysis was performed with a PALS Zeta Potential Analyzer Ver. 3.43 (Brookhaven Instruments Corp.). The X-ray powder diffraction (XRD) analysis was performed with a Japanese Rigaku D/max-cA rotating anode X-ray diffractometer equipped with monochromatic high-intensity Cu K_α radiation ($k = 0.1541874$ nm).

Preparation of HRP-Ab_2-AuNP/C Bioconjugates: At room temperature, 30 μL of 5.0 mg mL^{-1} HRP-Ab_2 was added to 5.0 mL of the AuNP/C composite solution prepared above. The mixture was gently mixed for 2 h, and centrifuged at 10 000 rpm for 20 min at 4 °C. After centrifugation, the oiled drop was washed with washing buffer and resuspended in 500 μL of PBST (PBS, 0.05% Tween) that contained 0.1% BSA as the assay solution. The spectrophotometric measurement at 280 nm was used to monitor the concentrations of the HRP-Ab_2 solutions before and after the assembly process. The decreases in absorbance of the solutions were applied to quantify the loading amount of HRP-Ab_2 bound to the AuNP/C composites.

Preparation of Soluble PDDA-CNTs (PDCNTs): CNTs were chemically shortened by ultrasonic agitation in a mixture of sulfuric acid and nitric acid (3: 1) for 3 h. The resulting CNTs were separated and washed repeatedly with distilled water by centrifugation until pH ~7. The purified CNTs were functionalized with PDDA according to the following procedures: 0.5 mg mL^{-1} of CNTs were dispersed into a 0.20% PDDA aqueous solution that contained 0.5 M NaCl and the resulting dispersion was sonicated for 30 min to give a homogeneous black suspension. Residual PDDA polymer was removed by high-speed centrifugation and the complex was rinsed with water at least three times. The collected complex was redispersed in water with mild sonicating to produce a stable solution of the complex, which was sonicated for 5 min immediately before preparing the films.

Preparation of Ab_1/PAA/PDCNT-Modified Immunosensor: The GCE with a diameter of 3 mm was used as the substrate to grow the GNP/PDCNT film. Prior to the preparation procedure of the films, the GCE was successively polished to a mirror finish using a 0.3 and 0.05 μm alumina slurry (Beuhler) followed by rinsing thoroughly with water. After successive sonication in 1: 1 nitric acid/water, acetone, and doubly distilled water, the electrode was rinsed with doubly distilled water and allowed to dry at room temperature. The PDCNT solution (4 μL of 5.0 mg mL^{-1}) was dropped on the pretreated GCE and dried in a silica gel desiccator, and then immersed in a 500 μL 1% PAA solution for 30 min. After the modified PAA/PDCNT/GCE was thoroughly rinsed with water, the electrode was subsequently immersed in a solution that contained 5×10^{-3} M EDC and 8×10^{-3} M NHS for 1 h. After the activated PAA/PDCNT/GCE was thoroughly rinsed with water, it was immersed immediately into a mixture of 60 μL of 0.2 mg mL^{-1} Ab_1 solution for 2 h to yield an Ab_1/PAA/PDCNT-modified GCE. The immunosensor obtained was stored in pH 7.0 PBS at 4 °C.

Immunoreaction Procedure and Measurement Procedure: The Ab_1-modified immunosensor was blocked with 100 μL of a 0.1 M triethanolamine solution for 1 h at room temperature, and washed with PBST. After aspiration, the Ab_1-modified electrodes were incubated with 60 μL of detecting Ag samples for 50 min at 37 °C. By the binding reaction between Ab_1 and Ag, the electrodes were immersed in 60 μL of a 1: 5 diluted HRP-Ab_2-AuNP/C bioconjugate solution or HRP-Ab_2 (1: 500) for an incubation period of 50 min. Finally, the electrodes were washed thoroughly with water to remove non-specifically bound conjugates, which could cause a background response before measurement. The method of the immobilization of Ab_1 and the immunoassay procedure are shown in Scheme 2.

The electrochemical impedance spectroscopy analyses were performed with an Autolab PGSTAT12 (Eco chemie, BV, The Netherlands) and controlled by GPES 4.9 and FRA 4.9 software. The electrochemical impedance spectra were recorded in the frequency range of $(0.1–1.0) \times 10^5$ Hz, at the formal potential of the $[Fe(CN)_6]^{3-/4-}$ redox couple and with a perturbation potential of 5 mV. Electrochemical immunoassay measurements were performed on a CHI 660 electrochemical analyzer (Co. CHI, USA) with a conventional three-electrode system comprised of platinum wire as the auxiliary electrode, a saturated calomel electrode (SCE) as the reference, and a modified GCE as the working electrode. The immunosensor was then placed in an electrochemical cell that contained 3.0 mL of pH 7.0 PBS buffer, 2.0×10^{-3} M *o*-phenylenediamine, and 4.0×10^{-3} M H_2O_2, which was deaerated thoroughly with high purity nitrogen for 5 min and maintained in a nitrogen atmosphere at room temperature. The differential pulse voltammetric measurements were performed from −0.3 to −0.8 V with a pulse amplitude of 50 mV and a pulse width of 50 ms.

Received: November 17, 2007
Revised: February 8, 2008
Published online: July 14, 2008

[1] J. Wang, *Small* **2005**, *1*, 1036.
[2] M. C. Daniel, D. Astruc, *Chem. Rev.* **2004**, *104*, 293.

[3] R. J. Cui, H.-C. Pan, J.-J. Zhu, H.-Y. Chen, *Anal. Chem.* **2007**, *79*, 8494.
[4] M. Dequairem, C. Degrand, B. Limoges, *Anal. Chem.* **2000**, *72*, 5521.
[5] L. Authier, C. Grossiord, P. Brossier, B. Limoges, *Anal. Chem.* **2001**, *73*, 4450.
[6] J. Wang, G. Liu, M. Rasul, *J. Am. Chem. Soc.* **2003**, *126*, 3010.
[7] X. Yu, B. Munge, V. Patel, G. Jensen, A. Bhirde, J. D. Gong, S. N. Kim, J. Gillespie, J. S. Gutkind, F. Papadimitrakopoulos, J. F. Rusling, *J. Am. Chem. Soc.* **2006**, *128*, 11 199.
[8] X. W. Zhao, Z. B. Liu, H. Yang, K. Nagai, Y. H. Zhao, Z. Z. Gu, *Chem. Mater.* **2006**, *18*, 2443.
[9] T. Deng, J.-S. Li, J.-H. Jiang, G.-L. Shen, R.-Q. Yu, *Adv. Funct. Mater.* **2006**, *16*, 2147.
[10] J. G. Huang, C. L. Lee, H.-M. Lin, T.-L. Chuang, W.-S. Wang, R.-H. Juang, C.-H. Wang, C. K. Lee, S.-M. Lin, C.-W. Lin, *Biosens. Bioelectron.* **2006**, *22*, 519.
[11] J. Wang, G. Liu, M. H. Engelhard, Y. Lin, *Anal. Chem.* **2006**, *78*, 6974.
[12] F. Caruso, *Top. Curr. Chem.* **2003**, *227*, 145.
[13] F. Caruso, R. A. Caruso, H. M. Hwald, *Science* **1998**, *282*, 1111.
[14] F. Caruso, *Adv. Mater.* **2001**, *13*, 11.
[15] D. Y. Wang, A. L. Rogach, F. Caruso, *Nano Lett.* **2002**, *2*, 857.
[16] X. M. Sun, Y. D. Li, *Angew. Chem.* **2004**, *116*, 607.
[17] H. Grisaru, O. Palchik, A. Gedanken, M. A. Slifkin, A. M. Weiss, V. Palchik, *Inorg. Chem.* **2003**, *42*, 7148.
[18] H. Grisaru, O. Palchik, A. Gedanken, V. Palchik, M. A. Slifkin, A. M. Weiss, Y. R. Hacohen, *Inorg. Chem.* **2001**, *40*, 4814.
[19] T. Sakaki, M. Shibata, T. Miki, H. Hirosue, N. Hayashi, *Bioresour. Technol.* **1996**, *58*, 197.
[20] D. Caruntu, B. L. Cushing, G. Caruntu, C. J. O'Connor, *Chem. Mater.* **2005**, *17*, 3398.
[21] X. Hong, J. Li, M. Wang, J. Xu, W. Guo, J. H. Li, Y. B. Bai, T. Li, *Chem. Mater.* **2004**, *16*, 4022.
[22] C. Guarize, L. Pasquato, P. Scrimin, *Langmuir* **2005**, *21*, 5537.
[23] K. G. Thomas, S. Barazzouk, B. I. Ipe, S. T. S. Joseph, P. V. Kamat, *J. Phys. Chem. B* **2004**, *108*, 13 066.
[24] *Colloidal Gold: Principles, Methods and Applications* (Ed.: M. A. Hayat), Academic Press, New York **1989**, p. 105.
[25] *Detection Techniques in Immunology* (Ed.: Y. W. Xu), Science Press, Beijing **1997**, p. 304.
[26] A. J. Bard, L. R. Faulkner, *Electrochemical Methods: Fundamentals and Applications*, Wiley, New York **1980**.
[27] R. Pei, Z. Cheng, E. Wang, X. Yang, *Biosens. Bioelectron.* **2001**, *16*, 355.
[28] J. Zhao, R. W. Henkens, J. Stonehuerner, J. P. O'Daly, A. L. Crumbliss, *J. Electroanal. Chem.* **1992**, *327*, 109.
[29] P. Scuderi, K. E. Sterling, K. S. Lam, P. R. Finley, K. J. Ryan, C. G. Ray, E. Petersen, D. J. Slymen, S. E. Salmon, *Lancet* **1986**, *2*, 1364.
[30] Y.-L. Zhang, Y. Huang, J.-H. Jiang, G.-L. Shen, R.-Q. Yu, *J. Am. Chem. Soc.* **2007**, *129*, 15 448.
[31] P. Kavanagh, D. Leech, *Anal. Chem.* **2006**, *78*, 2710.
[32] J. Das, K. Jo, J. W. Lee, H. Yang, *Anal. Chem.* **2007**, *79*, 2790.
[33] W. C. Mak, K. Y. Cheung, D. Trau, A. Warsinke, F. Scheller, R. Renneberg, *Anal. Chem.* **2005**, *77*, 2835.
[34] J. Turkevich, P. C. Stevenson, J. Hiller, *Faraday Discuss.* **1951**, *11*, 55.